Seismic data interpolation beyond aliasing using regularized nonstationary autoregression[a]

[a]Published in Geophysics, 76, V69-V77, (2011)

Yang Liu[*], *Sergey Fomel*[†]

ABSTRACT

Seismic data are often inadequately or irregularly sampled along spatial axes. Irregular sampling can produce artifacts in seismic imaging results. We present a new approach to interpolate aliased seismic data based on adaptive prediction-error filtering (PEF) and regularized nonstationary autoregression. Instead of cutting data into overlapping windows (patching), a popular method for handling nonstationarity, we obtain smoothly nonstationary PEF coefficients by solving a global regularized least-squares problem. We employ shaping regularization to control the smoothness of adaptive PEFs. Finding the interpolated traces can be treated as another linear least-squares problem, which solves for data values rather than filter coefficients. Compared with existing methods, the advantages of the proposed method include an intuitive selection of regularization parameters and fast iteration convergence. Benchmark synthetic and field data examples show that the proposed technique can successfully reconstruct data with decimated or missing traces.

INTRODUCTION

The regular and fine sampling along the time axis is common, whereas good spatial sampling is often more expensive or prohibitive and therefore is the main bottleneck for seismic resolution. Too large a spatial sampling interval may lead to aliasing problems that adversely affect the resolution of subsurface images. An alternative to expensive dense spatial sampling is interpolation of seismic traces. One important approach to trace interpolation is prediction interpolating methods (Spitz, 1991), which use low-frequency non-aliased data to extract antialiasing prediction-error filters (PEFs) and then interpolates high frequencies beyond aliasing. Claerbout (1992) extends Spitz's method using PEFs in the t-x domain. Porsani (1999) proposes a half-step PEF scheme that makes the interpolation process more efficient. Huard et al. (1996) and Wang (2002) extend f-x trace interpolation to higher spatial dimensions. Gulunay (2003) introduces an algorithm similar to f-x prediction filtering, which has an elegant representation in the f-k domain. Curry (2006) uses multidimensional nonstationary PEFs to interpolate diffracted multiples. Naghizadeh and Sacchi (2009) propose an adaptive f-x interpolation using exponentially weighted

recursive least squares. More recently, Naghizadeh and Sacchi (2010a) propose a prediction approach similar to Gulunay's method but using the curvelet transform instead of the Fourier transform. Abma and Kabir (2005) compare the performance of several different interpolation methods.

Correcting irregular spatial sampling is another application for seismic data interpolation algorithms. A variety of interpolation methods have been published in the recent years. One approach is to estimate the PEF on multiple rescaled copies of the irregular data (Curry, 2003), where the data are rescaled with a number of progressively-larger bin sizes. Curry (2004) further improves the rescaling method by introducing multiple scales of the data where the location of the grid cells are varied in addition to the size of the cells. Curry and Shan (2008) use pseudo-primary data by crosscorrelating multiples and primaries to estimate nonstationary PEF and then interpolated missing near offsets. Naghizadeh and Sacchi (2010b) propose autoregressive spectral estimates to reconstruct aliased data and data with gaps.

Seismic data are nonstationary. The standard PEF is designed under the assumption of stationary data and becomes less effective when this assumption is violated (Claerbout, 1992). Cutting data into overlapping windows (patching) is a common method to handle nonstationarity (Claerbout, 2010), although it occasionally fails in the presence of variable dips. Crawley et al. (1999) propose smoothly-varying nonstationary PEFs with "micropatches" and radial smoothing, which typically produces better results than the rectangular patching approach. Fomel (2002) develops a nonstationary plane-wave destruction (PWD) filter as an alternative to t-x PEF (Claerbout, 1992) and applies the PWD operator to trace interpolation. The PWD method depends on the assumption of a small number of smoothly variable seismic dips. Curry (2003) uses Laplacian and radial rougheners to ensure a nonstationary PEF that varies smoothly in space, which specifies an appropriate regularization operator.

In this paper, we use the two-step strategy, similar to that of Claerbout (1992) and Crawley et al. (1999), but calculate the adaptive PEF by using regularized nonstationary autoregression (Fomel, 2009) to handle both nonstationarity and aliasing. The key idea is the use of shaping regularization (Fomel, 2007) to constrain the spatial smoothness of filter coefficients. We provide an approach to nonstationary data interpolation, which has an intuitive selection of parameters and fast iteration convergence. We test the new method by using several benchmark synthetic examples. Results of applying the proposed method to a field data example demonstrate that it can be effective in trace interpolation problems, even in the presence of multiple strongly variable slopes.

THEORY

A common constraint for interpolating missing seismic traces is to ensure that the interpolated data, after specified filtering, have minimum energy (Claerbout, 1992).

Filtering is equivalent to spectral multiplication. Therefore, specified filtering is a way of prescribing a spectrum for the interpolated data. A sensible choice is a spectrum of the recorded data, which can be captured by finding the data's PEF (Spitz, 1991; Crawley, 2000). The PEF, also known as the autoregression filter, plays the role of the 'inverse-covariance matrix' in statistical estimation theory. A signal is regressed on itself in the estimation of PEF. The PEF can be implemented in either t-x (time-space) or f-x (frequency-space) domain. Time-space PEFs are less likely to create spurious events in the presence of noise than f-x PEFs (Abma, 1995; Crawley, 2000). When data interpolation is cast as an inverse problem, a PEF can be used to find missing data. This involves a two-step approach. In the first step, a PEF is estimated by minimizing the output of convolution of known data with an unknown PEF. In the second step, the missing data is found by minimizing the convolution of the recently calculated PEF with the unknown model, which is constrained where the data are known (Curry, 2004).

Step 1: Adaptive PEF estimation

Regular trace interpolation

An important property of PEFs is scale invariance, which allows estimation of PEF coefficients A_n (including the leading "-1" and prediction coefficients B_n) for incomplete aliased data $S(t,x)$ that include known traces $S_{known}(t,x_k)$ and unknown or zero traces $S_{zero}(t,x_z)$. For trace decimation, zero traces interlace known traces. To avoid zeroes that influence filter estimation, we interlace the filter coefficients with zeroes. For example, consider a 2-D PEF with seven prediction coefficients:

$$\begin{array}{ccccc} B_3 & B_4 & B_5 & B_6 & B_7 \\ \cdot & \cdot & -1 & B_1 & B_2 \end{array} \tag{1}$$

Here, the horizontal axis is time, the vertical axis is space, and "$\cdot$" denotes zero. Rescaling both time and spatial axes assumes that the dips represented by the original filter in equation 1 are the same as those represented by the scaled filter (Claerbout, 1992):

$$\begin{array}{ccccccccc} B_3 & \cdot & B_4 & \cdot & B_5 & \cdot & B_6 & \cdot & B_7 \\ \cdot & \cdot & \cdot & \cdot & \cdot & \cdot & \cdot & \cdot & \cdot \\ \cdot & \cdot & \cdot & \cdot & -1 & \cdot & B_1 & \cdot & B_2 \end{array} \tag{2}$$

For nonstationary situations, we can also assume locally stationary spectra of the data because trace decimation makes the space between known traces small enough, thus making adaptive PEFs locally scale-invariant. For estimating adaptive PEF coefficients, nonstationary autoregression allows coefficients B_n to change with both t and x. The new adaptive filter can look something like

$$\begin{array}{ccccccccc} B_3(t,x) & \cdot & B_4(t,x) & \cdot & B_5(t,x) & \cdot & B_6(t,x) & \cdot & B_7(t,x) \\ \cdot & \cdot & \cdot & \cdot & \cdot & \cdot & \cdot & \cdot & \cdot \\ \cdot & \cdot & \cdot & \cdot & -1 & \cdot & B_1(t,x) & \cdot & B_2(t,x) \end{array} \tag{3}$$

In other words, prediction coefficients $B_n(t,x)$ are obtained by solving the least-squares problem,

$$\begin{aligned}\widehat{B_n}(t,x) &= \arg\min_{B_n} \|S(t,x) - \sum_{n=1}^{N} B_n(t,x) S_n(t,x)\|_2^2 \\ &\quad +\epsilon^2 \sum_{n=1}^{N} \|\mathbf{D}[B_n(t,x)]\|_2^2 \,, \end{aligned} \tag{4}$$

where $S_n(t,x)$=$S(t - m\,i\,\Delta\,t, x - m\,j\,\Delta\,x)$, which represents the causal translation of $S(t,x)$, with time-shift index i and spatial-shift index j scaled by decimation interval m. Note that predefined constant m uses the interlacing value as an interval; i.e., the shift interval equals 2 in equation 3. Subscript n is the general shift index for both time and space, and the total number of i and j is N. $\mathbf{D}$ is the regularization operator, and ϵ is a scalar regularization parameter. All coefficients $B_n(t,x)$ are estimated simultaneously in a time/space variant manner. This approach was described by Fomel (2009) as regularized nonstationary autoregression (RNA). If $\mathbf{D}$ is a linear operator, least-squares estimation reduces to linear inversion

$$\mathbf{b} = \mathbf{A}^{-1}\,\mathbf{d}\,, \tag{5}$$

where

$$\mathbf{b} = \left[\begin{array}{cccc} B_1(t,x) & B_2(t,x) & \cdots & B_N(t,x) \end{array}\right]^T \,, \tag{6}$$

$$\mathbf{d} = \left[\begin{array}{cccc} S_1(t,x)\,S(t,x) & S_2(t,x)\,S(t,x) & \cdots & S_N(t,x)\,S(t,x) \end{array}\right]^T \,, \tag{7}$$

and the elements of matrix $\mathbf{A}$ are

$$A_{nk}(t,x) = S_n(t,x)\,S_k(t,x) + \epsilon^2\,\delta_{nk}\,\mathbf{D}^T\,\mathbf{D}\,. \tag{8}$$

Shaping regularization (Fomel, 2007) incorporates a shaping (smoothing) operator $\mathbf{G}$ instead of $\mathbf{D}$ and provides better numerical properties than Tikhonov's regularization (Tikhonov, 1963) in equation 4 (Fomel, 2009). Inversion using shaping regularization takes the form

$$\mathbf{b} = \widehat{\mathbf{A}}^{-1}\,\widehat{\mathbf{d}}\,, \tag{9}$$

where

$$\widehat{\mathbf{d}} = \left[\begin{array}{cccc} \mathbf{G}\left[S_1(t,x)\,S(t,x)\right] & \mathbf{G}\left[S_2(t,x)\,S(t,x)\right] & \cdots & \mathbf{G}\left[S_N(t,x)\,S(t,x)\right] \end{array}\right]^T \,, \tag{10}$$

the elements of matrix $\widehat{\mathbf{A}}$ are

$$\widehat{A}_{nk}(t,x) = \lambda^2\,\delta_{nk} + \mathbf{G}\left[S_n(t,x)\,S_k(t,x) - \lambda^2\,\delta_{nk}\right] \,, \tag{11}$$

and λ is a scaling coefficient. One advantage of the shaping approach is the relative ease of controlling the selection of λ and $\mathbf{G}$ in comparison with ϵ and $\mathbf{D}$. We define $\mathbf{G}$ as Gaussian smoothing with an adjustable radius, which is designed by repeated application of triangle smoothing (Fomel, 2007), and choose λ to be the mean value of $S_n(t,x)$.

Coefficients $B_n(t,x_z)$ at zero traces $S_{zero}(t,x_z)$ get constrained (effectively smoothly interpolated) by regularization. The required parameters are the size and shape of the filter $B_n(t,x)$ and the smoothing radius in $\mathbf{G}$.

Missing data interpolation

Irregular gaps occur in the recorded data for many different reasons, and prediction-error filters are known to be a powerful method for interpolating missing data. Missing data interpolation is a particular case of data regularization, where the input data are already given on a regular grid, and one needs to reconstruct only the missing values in empty bins (Fomel, 2001). One can use existing traces to directly estimate adaptive PEF coefficients instead of scaling the filter as in regular trace interpolation problem. However, finding the adaptive PEF needs to avoid using any regression equations that involve boundaries or missing data. This can be achieved by creating selection mask operator $K(t,x)$, a diagonal matrix with ones at the known data locations and zeros elsewhere, for both causal translations and input data (Claerbout, 2010).

Analogously to the stationary prediction-error filter (1), adaptive PEF coefficients $B_n(t,x)$ use the unscaled format and appear as

$$\begin{array}{ccccc} B_3(t,x) & B_4(t,x) & B_5(t,x) & B_6(t,x) & B_7(t,x) \\ \cdot & \cdot & -1 & B_1(t,x) & B_2(t,x) \end{array} \tag{12}$$

The nonstationary coefficients $B_n(t,x)$ can be obtained by solving the least-squares problem

$$\begin{aligned} \widehat{B_n}(t,x) &= \arg\min_{B_n} \|K(t,x)[S(t,x) - \sum_{n=1}^{N} B_n(t,x) S_n(t,x)]\|_2^2 \\ &\quad + \epsilon^2 \sum_{n=1}^{N} \|\mathbf{D}[B_n(t,x)]\|_2^2 \; . \end{aligned} \tag{13}$$

where $S_n(t,x) = S(t-i, x-j)$. By using shaping regularization, adaptive PEF coefficients are smoothly filled at missing trace locations.

Step 2: Data interpolation with adaptive PEF

In the second step, a similar problem is solved, except that the filter is known, and the missing traces are unknown. In the decimated-trace interpolation problem, we squeeze (by throwing away alternate zeroed rows and columns) the filter in equation 3 to its original size and then formulate the least-squares problem,

$$\widehat{S}(t,x) = \arg\min_{S} \|S(t,x) - \sum_{n=1}^{N} \widehat{B_n}(t,x) S_n(t,x)\|_2^2 \; , \tag{14}$$

subject to

$$\widehat{S}(t,x_k) = S_{known}(t,x_k) \; , \tag{15}$$

where $\widehat{S}(t,x)$ represents the interpolated output, and i and j use the original shift as the interval; i.e., the shift interval equals 1.

We carry out the minimization in equations 4, 13, and 14 by the conjugate gradient method (Hestenes and Stiefel, 1952). The constraint condition (equation 15) is used as the initial model and constrains the output by using the known traces for each iteration in the conjugate-gradient scheme. The computational cost is proportional to $N_{iter} \times N_f \times N_t \times N_x$, where N_{iter} is the number of iterations, N_f is the filter size, and $N_t \times N_x$ is the data size. In our tests, N_f and N_{iter} were approximately equal to 100. Increasing the smoothing radius in shaping regularization decreases N_{iter} in the filter estimation step.

SYNTHETIC DATA TESTS

Aliasing decimated-trace interpolation test

We start with a strongly aliased synthetic example from Claerbout (2009). The sparse spatial sampling makes the gather severely aliased, especially at the far offset positions (Figure 1a). For comparison, we used PWD (Fomel, 2002) to interpolate the traces (Figure 1b). Interpolation with PWD depends on dip estimation. In this example, the true dip is non-negative everywhere and is easily distinguished from the aliased one. Therefore, the PWD method recovers the interpolated traces well. However, in the more general case, an additional interpretation may be required to determine which of the dip components is contaminated by aliasing. According to the theory described in the previous section, the PEF-based methods use the lower (less aliased) frequencies to estimate PEF coefficients, and then interpolate the decimated traces (high-frequency information) by minimizing the convolution of the scale-invariant PEF with the unknown model, which is constrained where the data is known. We designed adaptive PEFs using 10 (time) $\times$ 2 (space) coefficients for each sample and a 50-sample (time) $\times$ 2-sample (space) smoothing radius and then applied them so as to interpolate the aliased trace. The nonstationary autoregression algorithm effectively removes all spatial aliasing artifacts (Figure 1c). The proposed method compares well with the PWD method. The CPU times, for single 2.66GHz CPU used in this example, are 20 seconds for adaptive PEF estimation (step 1) and 2 seconds for data interpolation (step 2).

Abma decimated-trace interpolation tests

A benchmark example created by Raymond Abma (personal communication) shows a simple curved event (Figure 2a). The challenge in this example is to account for both nonstationarity and aliasing. Figure 2b shows the interpolated result using Claerbout's stationary t-x PEF, which was estimated and applied in one big window, with each PEF coefficient B_n constant at every data location. Note that the t-x PEF method can recover the aliasing trace only in the dominant slope range. The trace-interpolating result using regularized nonstationary autoregression is shown in Figure 2c. The adaptive PEF has 20 (time) $\times$ 3 (space) coefficients for each sample

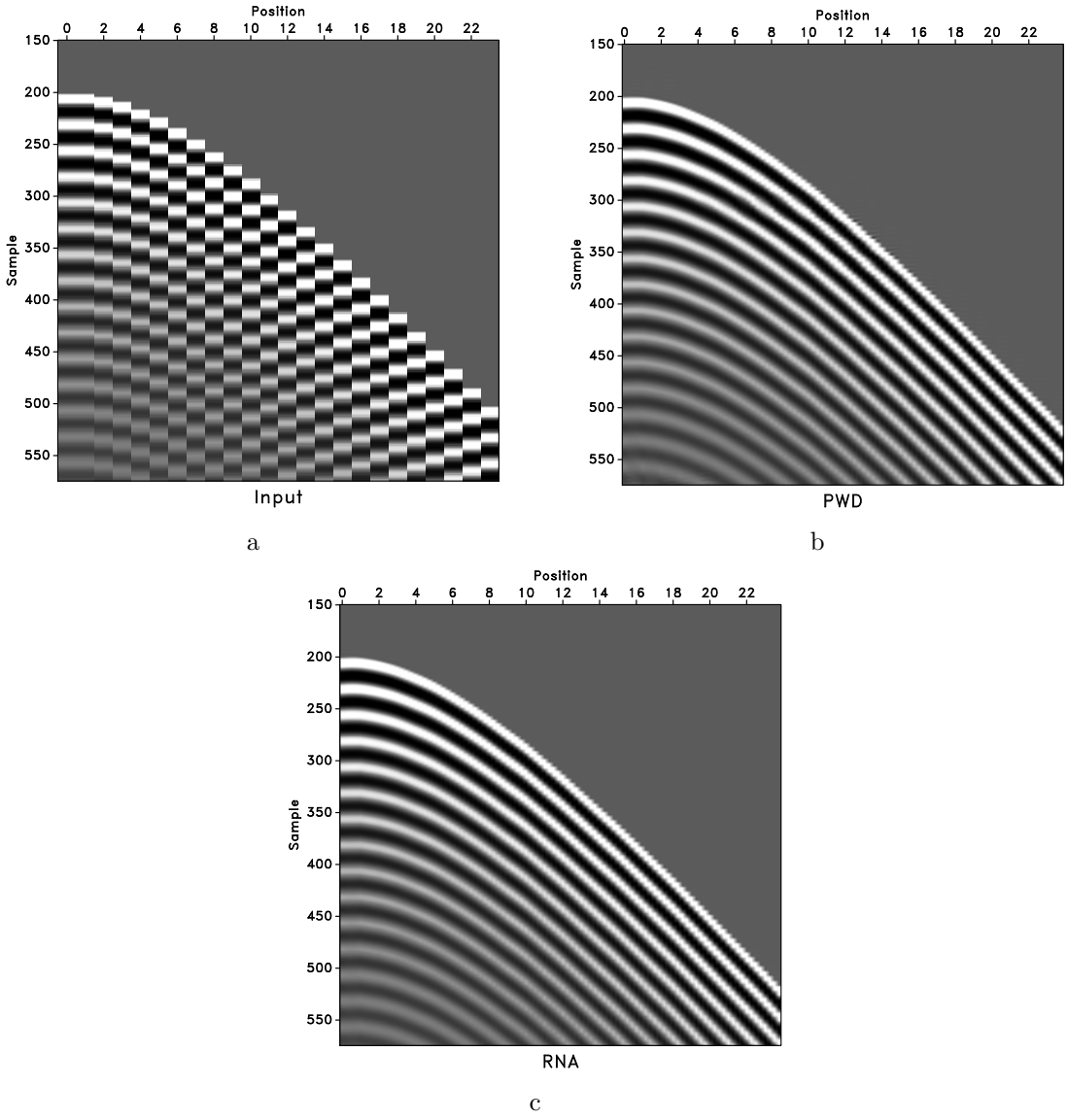

Figure 1: Aliased synthetic data (a), trace interpolation with plane-wave destruction (b), and trace interpolation with regularized nonstationary autoregression (c). Three additional traces were inserted between each of the neighboring input traces.

and a 20-sample (time) × 3-sample (space) smoothing radius. The proposed method eliminates all nonstationary aliasing and improves the continuity of the curved event.

Abma and Kabir (2005) present a comparison of several algorithms used for trace interpolation. We chose the most challenging benchmark Marmousi example from Abma and Kabir to illustrate the performance of RNA interpolation. Figure 3a shows a zero-offset section of the Marmousi model, in which curved events violate the assumptions common for most trace-interpolating methods. Figure 3b shows that our method produces reasonable results for both curved and weak events and does not introduce any undesirable noise. The adaptive PEF parameters correspond to 7 (time) × 5 (space) coefficients for each sample and a 40-sample (time) × 30-sample (space) smoothing radius.

Missing-trace interpolation test

A missing trace test is shown in Figure 4a and comes from decimated-trace interpolation result (Figure 2c) after removing 70% of randomly selected traces. The curved event makes it difficult to recover the missing traces. The interpolated result is shown in Figure 4b, which uses a regularized adaptive PEF with 4 (time) × 2 (space) coefficients for each sample and a 50-sample (time) × 10-sample (space) smoothing radius. In the interpolated result, it is visually difficult to distinguish the missing trace locations, which is an evidence of successful interpolation. The filter size along space direction needs to be small in order to generate enough regression equations.

FIELD DATA EXAMPLES

We use a set of marine 2-D shot gathers from a deepwater Gulf of Mexico survey (Crawley et al., 1999; Fomel, 2002) to further test the proposed method. Figure 5 shows the data before and after subsampling in the offset direction. The shot gather has long-period multiples and complicated diffraction events caused by a salt body. Amplitudes of the events are not uniformly distributed. Subsampling by a factor of 2 (Figure 5b) causes visible aliasing of the steeply dipping events. We designed a nonstationary PEF, with 15 (time) × 5 (space) coefficients for each sample and a 50-sample (time) × 20-sample (space) smoothing radius to handle the variability of events. Figure 6 shows the interpolation result and the difference between interpolated traces and original traces plotted at the same clip value. The proposed method succeeds in the sense that it is hard to distinguish interpolated traces from the interpolation result alone. A close-up comparison between the original and interpolated traces (Figure 7) shows some small imperfections. Some energy of the steepest events is partly missing. Coefficients of the adaptive PEF are illustrated in Figure 8, which displays the first coefficient (B_1) and the mean coefficient of B_n, respectively. The filter coefficients vary in time and space according to the curved events. The inter-

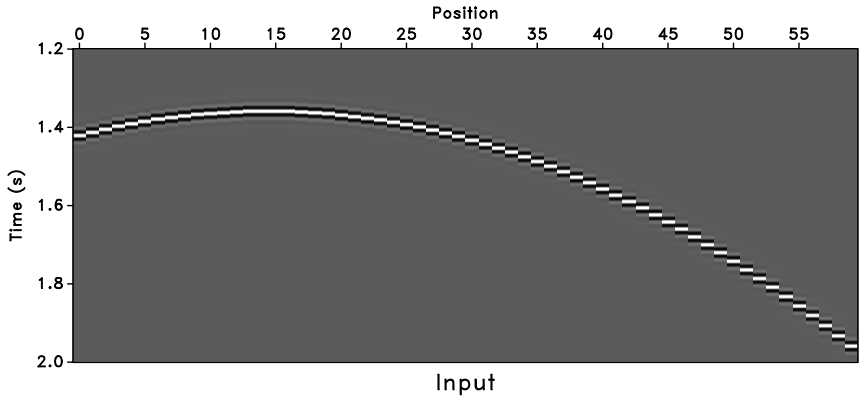

a

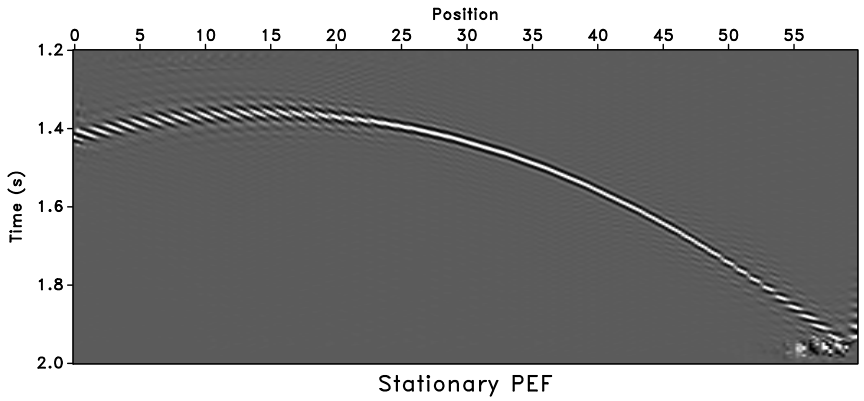

b

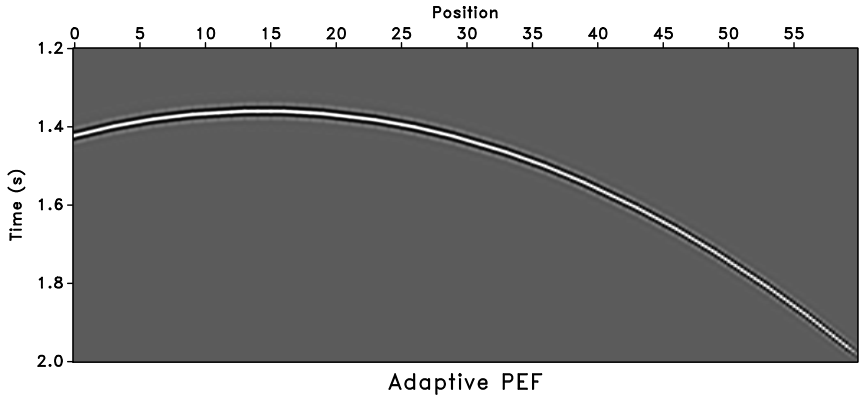

c

Figure 2: Curve model (a), trace interpolation with stationary PEF (b), and trace interpolation with adaptive PEF (c).

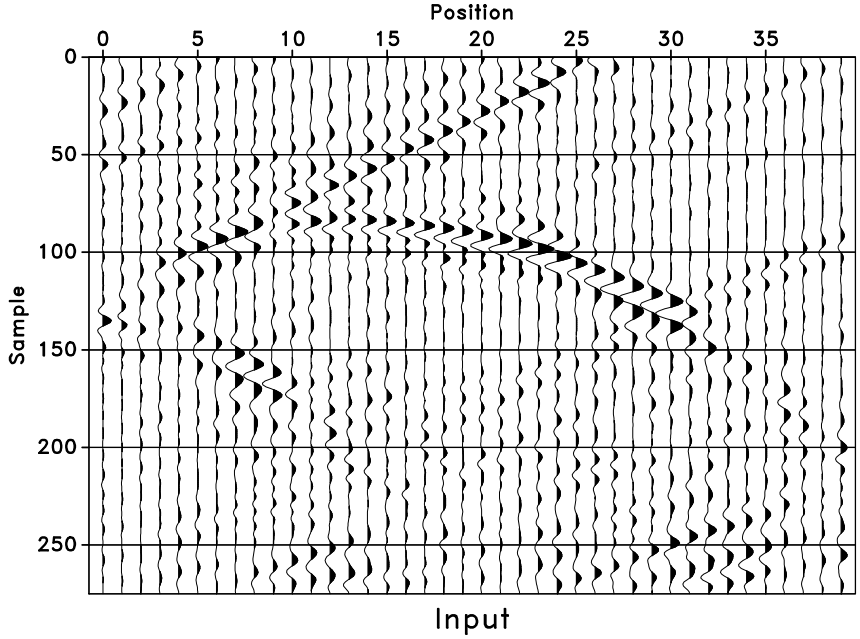

a

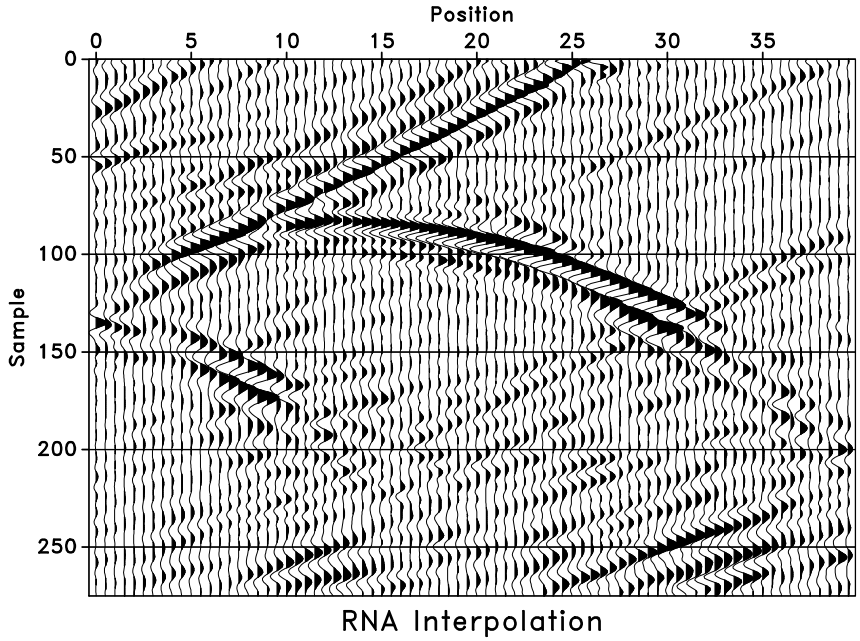

b

Figure 3: Marmousi model (a) and trace interpolation with regularized nonstationary autoregression (b).

a

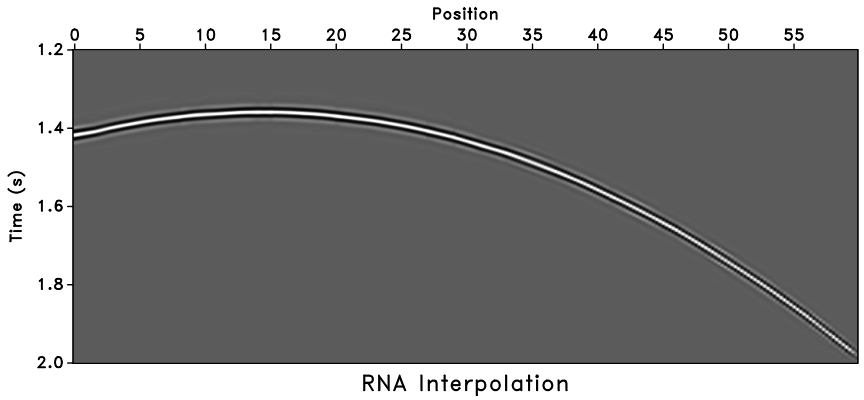

b

Figure 4: Curved model (Figure 2c) with 70% randomly selected traces removed (a) and trace interpolation with regularized nonstationary autoregression (b).

polated results are relatively insensitive to the smoothing parameters.

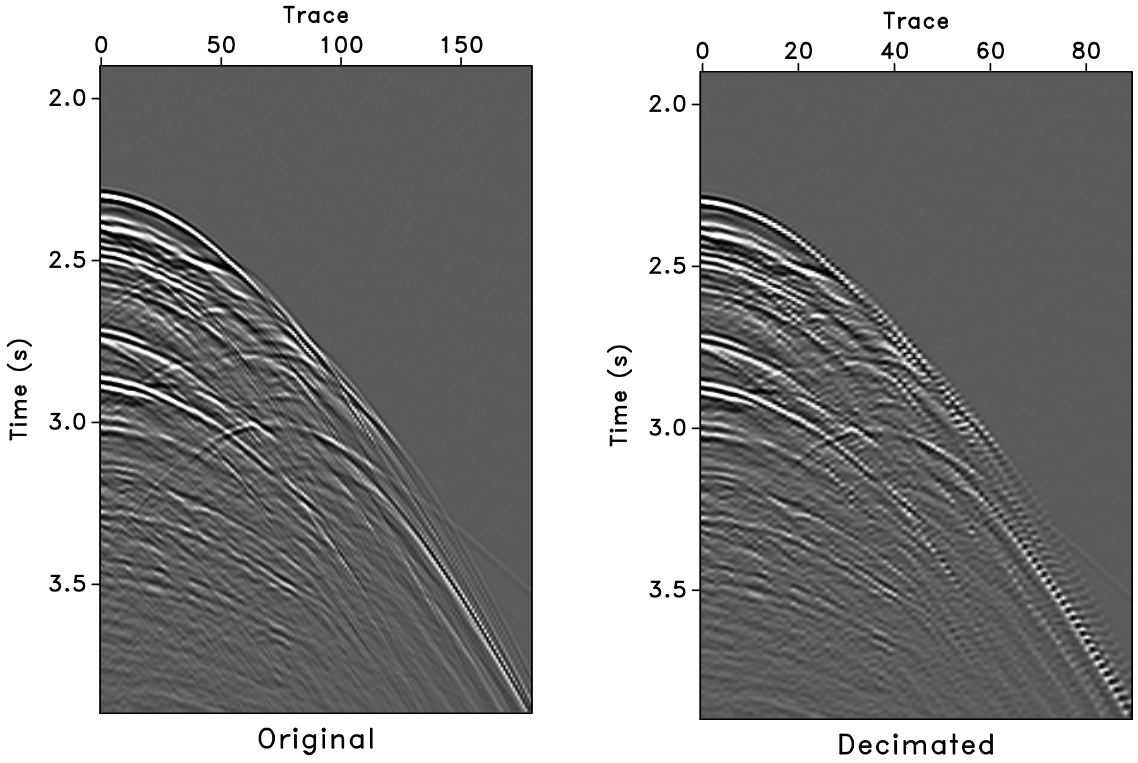

Figure 5: A 2-D marine shot gather. Original input (a) and input subsampled by a factor of 2 (b).

For a missing-trace interpolation test (Figure 9a), we removed 40% of randomly selected traces from the input data (Figure 5a). Furthermore, the first five traces were also removed to simulate traces missing at near offset. The adaptive PEF can only use a small number of coefficients in the spatial direction because of a small number of fitting equations (where the adaptive PEF lies entirely on known data). However, it also limits the ability of the proposed method to interpolate dipping events. We used a nonstationary PEF with 4 (time) $\times$ 3 (space) coefficients for each sample and a 50-sample (time) $\times$ 10-sample (space) smoothing radius to handle the missing trace recovery. The result is shown in Figure 9b. By comparing the results with the original input (Figure 5a), the missing traces are interpolated reasonably well except for weaker amplitude of the steeply dipping events.

An extension of the method to 3-D is straightforward and follows a two-step least-squares method with 3-D adaptive PEF estimation. We use a set of shot gathers as the input data volume to further test our method (Figure 10a). We removed 50% of randomly selected traces and five near offset traces for all shots (Figure 10b). For comparison, we used PWD to recover the missing traces (Figure 11a). The PWD method produces a reasonable result after carefully estimating dip information, but

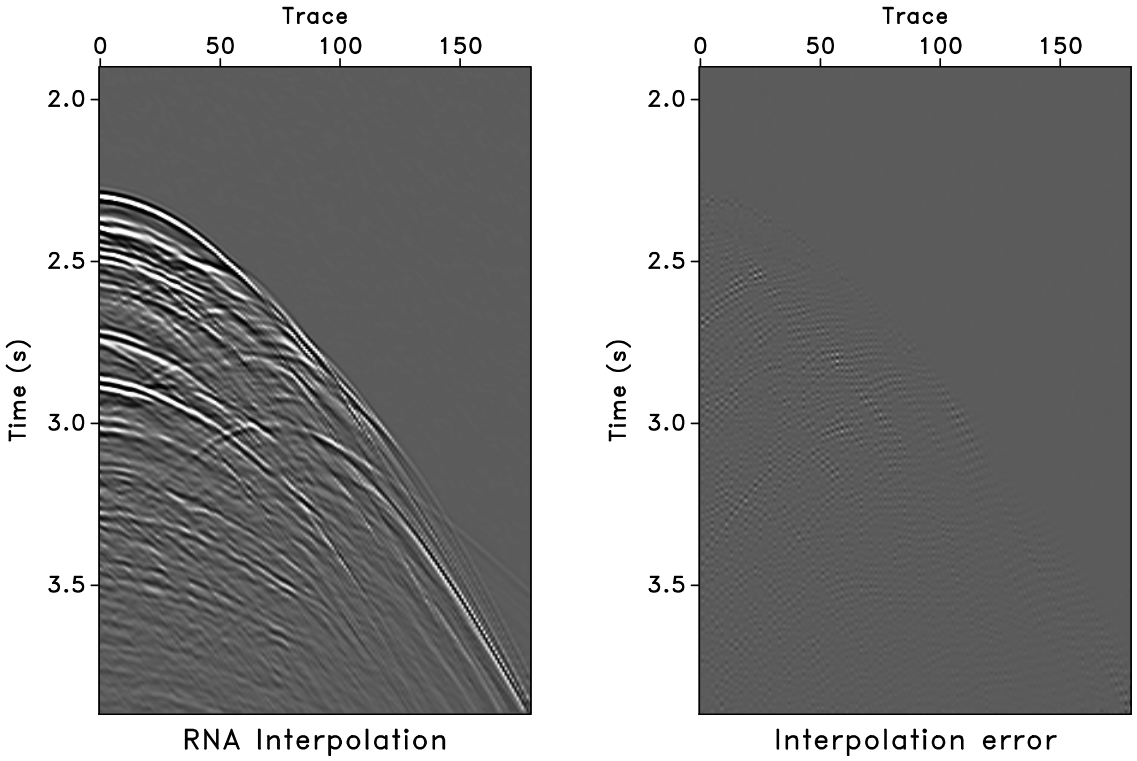

a b

Figure 6: Shot gather after trace interpolation (adaptive PEF with 15×5) (a) and difference between original gather (Figure 5a) and interpolated result (Figure 6a) (b).

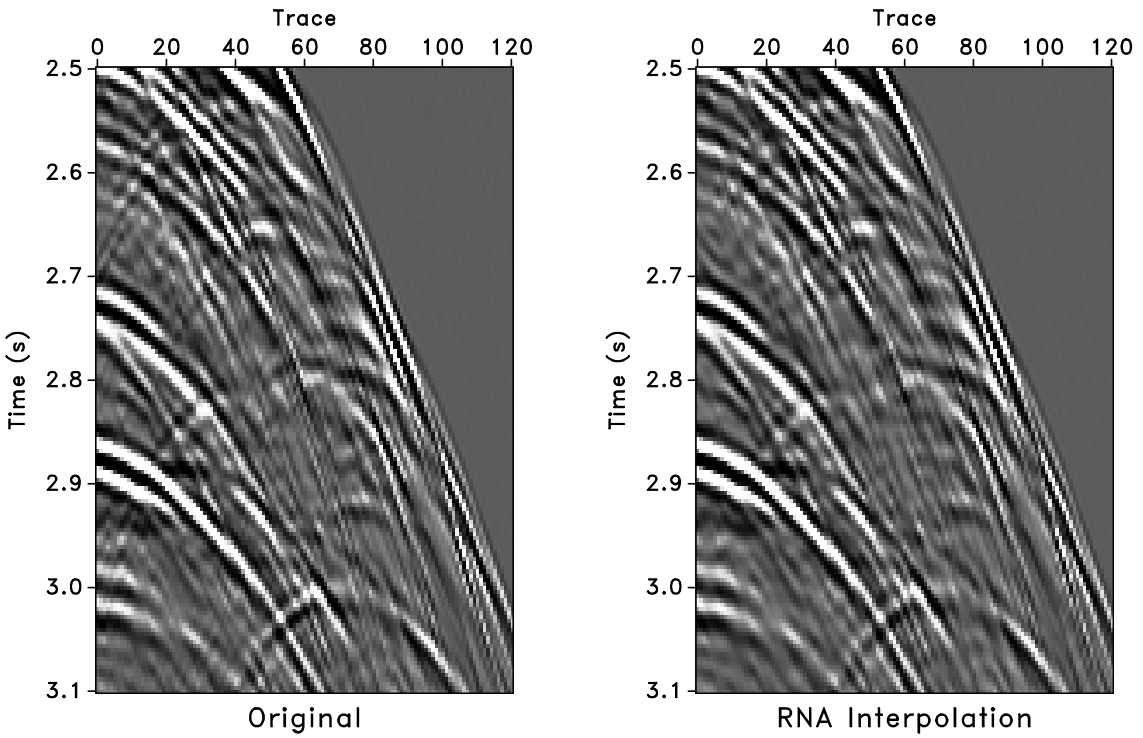

Figure 7: Close-up comparison of original data (a) and interpolated result by RNA (b).

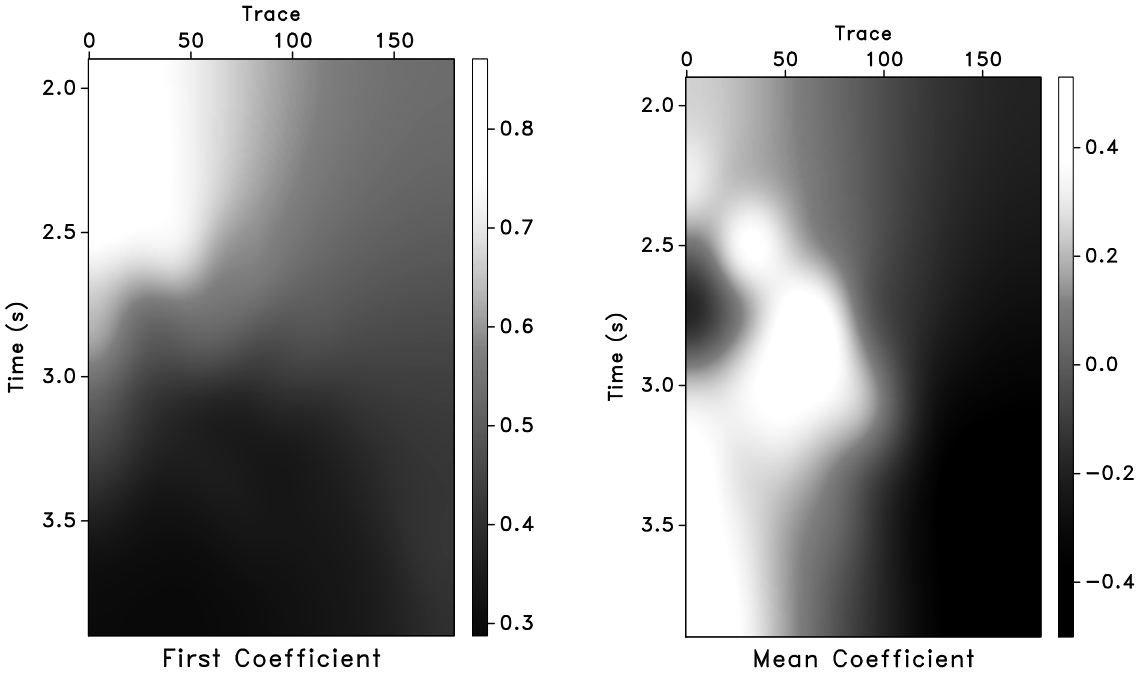

Figure 8: Adaptive PEF coefficients. First coefficient B_1 (a) and mean coefficient of B_n (b).

the interpolated error is slightly larger in the diffraction locations. (Figure 11b). The additional direction provided more information for interpolation but also increased the number of zeros in the mask operator $K(t, x)$, which constrains enough fitting equations in equation 13. To use the available fitting equations for adaptive PEF estimation, we chose a smaller number of coefficients in the spatial direction. The proposed method is able to handle conflicting dips, although it does not appear to improve the dipping-event recovery compared to the 2-D case. This characteristic partly limits the application of RNA in 3-D case. We used a 3-D nonstationary PEF with 4 (time) $\times$ 2 (space) $\times$ 2 (space) coefficients for each sample and a 50-sample (time) $\times$ 10-sample (space) $\times$ 10-sample (space) smoothing radius was selected. Similar to the result in the 2-D example, Figure 11c shows the interpolation result, in which only steeply-dipping low-amplitude diffraction events with are lost (Figure 11d).

CONCLUSIONS

We have introduced a new approach to adaptive prediction-error filtering for seismic data interpolation. Our approach uses regularized nonstationary autoregression to handle time-space variation of nonstationary seismic data. We apply this method to interpolating seismic traces beyond aliasing and to reconstructing data with missing and decimated traces. Experiments with benchmark synthetic examples and field

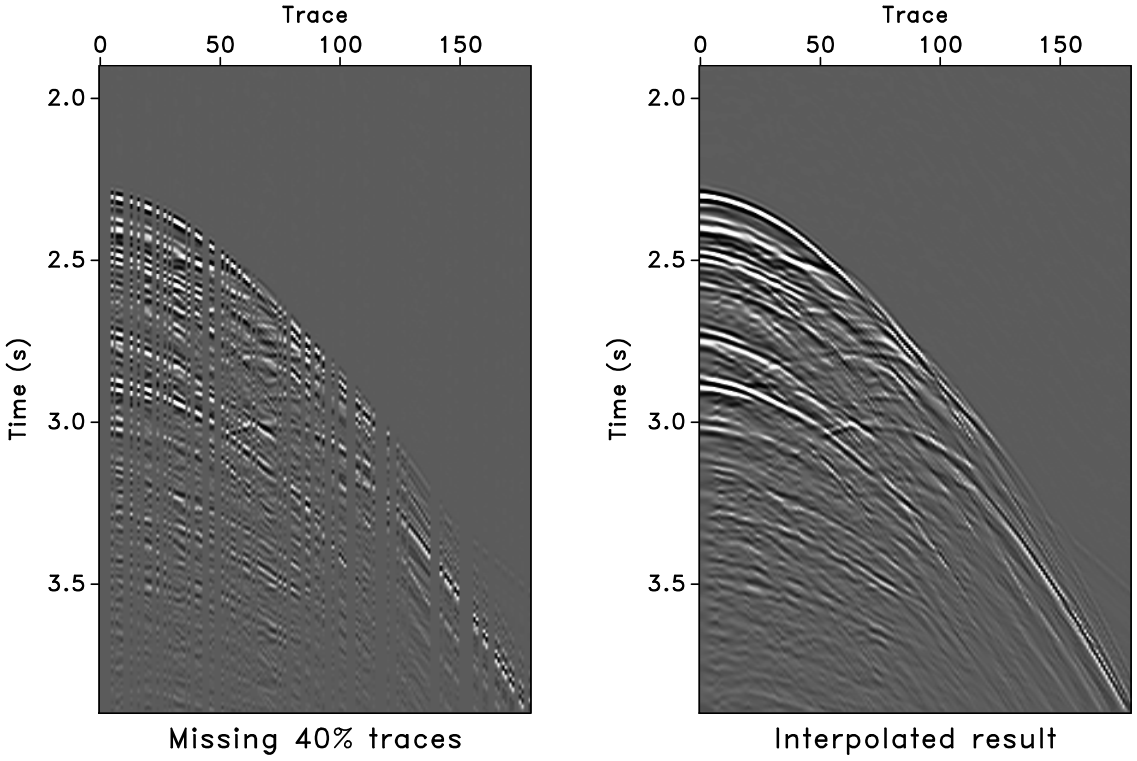

a b

Figure 9: Field data with 40% randomly missing traces (a), and reconstructed data using RNA (b).

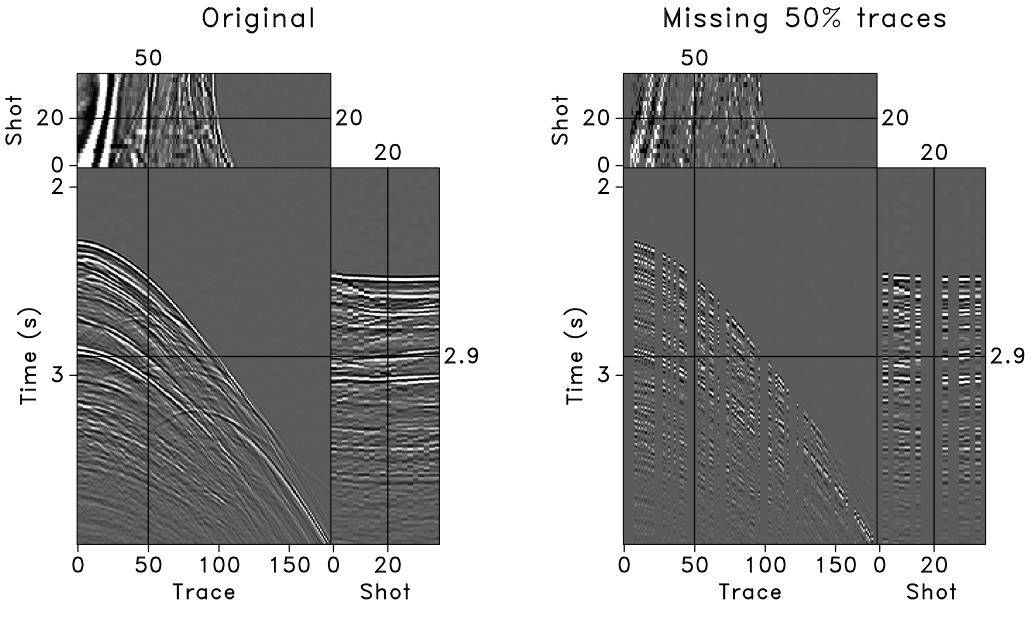

a b

Figure 10: A 3-D field data volume (a) and data with 50% randomly missing traces (b).

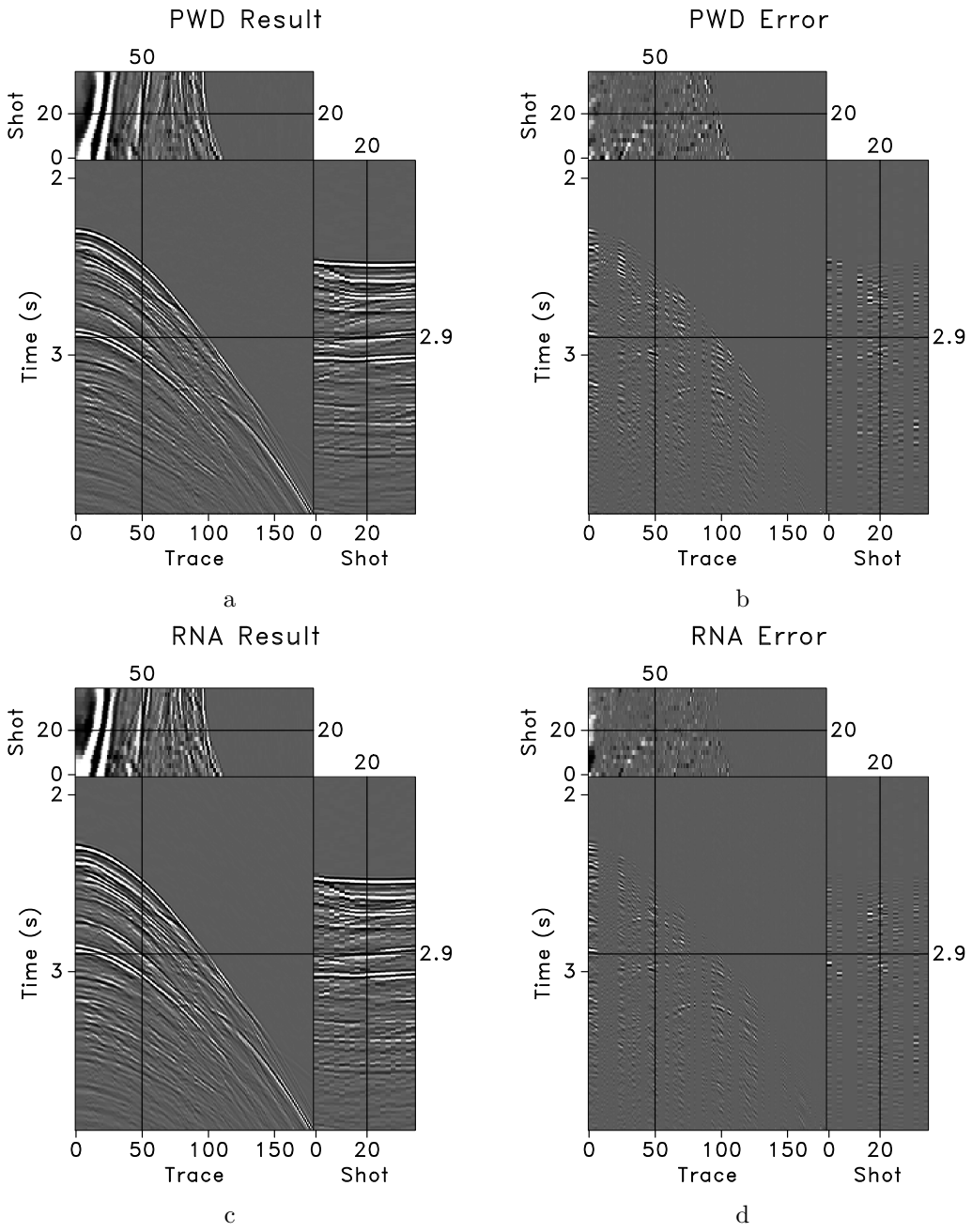

Figure 11: Reconstructed data volume using 3-D plane-wave destruction (a), difference between original input (Figure 10a) and interpolated result (Figure 11a), reconstructed data volume using 3-D regularized nonstationary autogression (c), and difference between original input (Figure 10a) and interpolated result (Figure 11c) (d).

data tests show that the proposed filters can depict nonstationary signal variation and provide a useful description of complex wavefields having multiple curved events. These properties are useful for applications such as seismic data interpolation and regularization. Other possible applications may include seismic noise attenuation.

ACKNOWLEDGMENTS

We are grateful to Raymond Abma for providing benchmark data sets. We thank Eric Verschuur, Bill Curry, and two anonymous reviewers for helpful suggestions, which improved the quality of the paper.

This publication was authorized by the Director, Bureau of Economic Geology, The University of Texas at Austin.

REFERENCES

Abma, R., 1995, Least-squares separation of signal and noise with multidimensional filters: PhD thesis, Stanford University.

Abma, R., and N. Kabir, 2005, Comparisons of interpolation methods: The Leading Edge, **24**, 984–989.

Claerbout, J. F., 1992, Earth Soundings Analysis: Processing Versus Inversion: Blackwell Scientific Publications.

———, 2009, Basic earth imaging: Stanford Exploration Project, `http://sepwww.stanford.edu/sep/prof/`.

———, 2010, Image estimation by example: Geophysical soundings image construction - Multidimensional autoregression: Stanford Exploration Project, http://sepwww.stanford.edu/sep/prof/.

Crawley, S., 2000, Seismic trace interpolation with nonstationary prediction-error filters: PhD thesis, Stanford University.

Crawley, S., J. Claerbout, and R. Clapp, 1999, Interpolation with smoothly nonstationary prediction-error filters: 69th Annual International Meeting, SEG, Expanded Abstracts, 1154–1157.

Curry, W., 2003, Interpolation of irregularly sampled data with nonstationary, multiscale prediction-error filters: 73th Annual International Meeting, SEG, Expanded Abstracts, 1913–1916.

———, 2004, Interpolation with multi-shifted-scale prediction-error filters: 74th Annual International Meeting, SEG, Expanded Abstracts, 2005–2008.

———, 2006, Interpolating diffracted multiples with prediction-error filters: 76th Annual International Meeting, SEG, Expanded Abstracts, 2709–2712.

Curry, W., and G. Shan, 2008, Interpolation of near offsets using multiples and prediction-error filters: 78th Annual International Meeting, SEG, Expanded Abstracts, 2421–2424.

Fomel, S., 2001, Three-dimensinal seismic data regularization: PhD thesis, Ph.D. thesis, Stanford University.

———, 2002, Applications of plane-wave destruction filters: Geophysics, **67**, 1946–1960.

———, 2007, Shaping regularization in geophysical-estimation problems: Geophysics, **72**, R29–R36.

———, 2009, Adaptive multiple subtraction using regularized nonstationary regression: Geophysics, **74**, V25–V33.

Gulunay, N., 2003, Seismic trace interpolation in the Fourier transform domain: Geophysics, **68**, 355–369.

Hestenes, M. R., and E. Stiefel, 1952, Methods of conjugate gradients for solving linear systems: Journal of Research of the National Bureau of Standards, **49**, 409–436.

Huard, I., S. Medina, and S. Spitz, 1996, F-XY wavefiedl de-aliasing for acquisition configurations leading to coarse sampling: 58th Annual International Meeting, EAGE, Expanded Abstracts, B039.

Naghizadeh, M., and M. D. Sacchi, 2009, f-x adaptive seismic-trace interpolation: Geophysics, **74**, V9–V16.

———, 2010a, Beyond alias hierarchical scale curvelet interpolation of regularly and irregularly sampled seismic data: Geophysics, **75**, WB189–WB202.

———, 2010b, Robust reconstruction of aliased data using autoregressive spectral estimates: Geophysical Prospecting, **58**, 1049–1062.

Porsani, M. J., 1999, Seismic trace interpolation using half-step prediction filters: Geophysics, **64**, 1461–1467.

Spitz, S., 1991, Seismic trace interpolation in the F-X domain: Geophysics, **56**, 785–794.

Tikhonov, A. N., 1963, Solution of Incorrectly Formulated Problems and the Regularization Method: Soviet Mathematics – Doklady.

Wang, Y., 2002, Seismic trace interpolation in the f-x-y domain: Geophysics, **67**, 1232–1239.